The Lowest Excited Singlet States of 1-Azaadamantane and 1-Azabicyclo[2.2.2]octane: Fluorescence Excitation Spectroscopy and Density Functional Calculations

ARTICLE *in* JOURNAL OF THE AMERICAN CHEMICAL SOCIETY · NOVEMBER 1997

Impact Factor: 12.11 · DOI: 10.1021/ja972411u

5 AUTHORS, INCLUDING:

Jurriaan M Zwier
Cisbio Bioassays
52 PUBLICATIONS **1,134** CITATIONS
SEE PROFILE

Albert M Brouwer
University of Amsterdam
142 PUBLICATIONS **3,408** CITATIONS
SEE PROFILE

Dick Bebelaar
University of Amsterdam
29 PUBLICATIONS **445** CITATIONS
SEE PROFILE

Wybren J Buma
University of Amsterdam
184 PUBLICATIONS **2,440** CITATIONS
SEE PROFILE

The Lowest Excited Singlet States of 1-Azaadamantane and 1-Azabicyclo[2.2.2]octane: Fluorescence Excitation Spectroscopy and Density Functional Calculations

Jurriaan M. Zwier,[†] Piet G. Wiering,[†] Albert M. Brouwer,*[,†] Dick Bebelaar,[‡] and Wybren Jan Buma*[,‡]

Contribution from the Amsterdam Institute of Molecular Studies, Laboratory of Organic Chemistry, University of Amsterdam, Nieuwe Achtergracht 129, 1018 WS Amsterdam, The Netherlands, and Laboratory for Physical Chemistry, University of Amsterdam, Nieuwe Achtergracht 127, 1018 WS Amsterdam, The Netherlands

Received July 17, 1997[⊗]

Abstract: The lowest excited singlet states of the structurally rigid amines 1-azaadamantane and 1-azabicyclo[2.2.2]-octane have been investigated by using fluorescence excitation spectroscopy on samples seeded in supersonic expansions. Based upon the notion that in both species the lowest excited singlet state is a Rydberg state with the ground state of the radical cation as its ionic core, excitation spectra have been analyzed by employing density functional calculations of the equilibrium geometries and force fields of the ground state of the neutral species and its radical cation. A good agreement is obtained between experimentally observed and theoretically predicted frequencies and intensities of vibronic transitions. Subsequent refinements of the geometry of the lowest excited singlet state are shown to account adequately for the minor differences between experiment and the computational results obtained by using the radical cation as a model for the lowest excited singlet state. From our analysis it also becomes apparent that the excited state is in both molecules subject to vibronic coupling with higher-lying excited states, as exemplified by the presence of transitions to non-totally symmetric vibrational levels. The results of the present study enable the determination of mode-specific reorganization energies accompanying ionization of 1-azaadamantane, which are shown to correspond qualitatively well with those determined in resonance Raman studies on the charge transfer transition in the electron donor−acceptor system **1**, which contains 1-azaadamantane as the electron donor unit.

I. Introduction

Geometry changes occurring in a molecular system undergoing an electronic transition play an important and often decisive role in determining the probability or rate of the process. High-resolution optical spectra obtained by absorption, emission, or resonance Raman spectroscopy can in principle be analyzed to yield these geometry changes in terms of displacements along the normal modes of vibration. The same vibrational overlap integrals that determine the spectral shapes also appear in the theoretical expressions for intramolecular electron transfer. In the most commonly used theories of electron transfer,[1] the complete multidimensional set of Franck−Condon factors is replaced by one factor involving a single "average" mode that accounts for all of the internal reorganization energy and a classical factor replacing low-frequency modes, including solvent reorganization. For many systems it has been attempted to obtain intramolecular reorganization energies from the analysis of optical absorption and emission spectra and from electron transfer rates, modulated by internal and external variables.[2−6] The theoretical description of these observables also includes, however, other parameters involved in the charge transfer process, in particular the thermodynamic driving force, electronic couplings, and the external (solvent) reorganization energy. Unfortunately, in most cases the experimental data do not permit an unambiguous separation of the individual parameters. In principle, resonance Raman spectroscopy (in combination with absorption and emission spectra) allows the determination of the frequencies and displacements necessary to evaluate the full multimode rate expressions. With this idea in mind, Myers and her group have recently investigated[7,8] the intramolecular electron-donor−acceptor (EDA) system **1** (see Figure 1), first synthesized and studied in the early seventies by Verhoeven and co-workers.[9,10] Several vibrational modes could be specifically attributed to donor or acceptor units, and mode-specific reorganization energies were reported.

It is usually assumed that the ground electronic state of an EDA system such as **1** has very little charge-transfer (CT) character, while the excited state can be described as an ion pair: $D^{\bullet+}$-bridge-$A^{\bullet-}$. This implies that accurate studies of (mode specific) internal reorganization energies might be performed by investigating the individual donor and acceptor components. Considering the donor part of the system, this would amount to determining the changes in molecular geometry

[†] Laboratory of Organic Chemistry.
[‡] Laboratory for Physical Chemistry.
[⊗] Abstract published in *Advance ACS Abstracts,* November 1, 1997.

(1) Brunschwig, B. S.; Sutin, N. *Comments Inorg. Chem.* **1987**, *6,* 209.
(2) Claude, J. P.; Williams, D. S.; Meyer, T. J. *J. Am. Chem. Soc.* **1996**, *118,* 9782.
(3) Gould, I. R.; Ege, D.; Moser, J. E.; Farid, S. *J. Am. Chem. Soc.* **1990**, *112,* 4290.
(4) Gould, I. R.; Noukakis, D.; Gomez-Jahn, L.; Goodman, J. L.; Farid, S. *J. Am. Chem. Soc.* **1993**, *115,* 4405.
(5) Katz, N. E.; Mecklenburg, S. L.; Graff, D. K.; Chen, P. Y.; Meyer, T. J. *J. Phys. Chem.* **1994**, *98,* 8959.
(6) Zeng, Y.; Zimmt, M. B. *J. Phys. Chem.* **1992**, *96,* 8395.
(7) Phillips, D. L.; Gould, I. R.; Verhoeven, J. W.; Tittelbach-Helmrich, D.; Myers, A. B. *Chem. Phys. Lett.* **1996**, *258,* 87.
(8) Lilichenko, M.; Verhoeven, J. W.; Myers, A. B. Submitted for publication.
(9) Dekkers, A. W. J. D.; Verhoeven, J. W.; Speckamp, W. N. *Tetrahedron* **1973**, *29,* 1691.
(10) Worrell, C.; Verhoeven, J. W.; Speckamp, W. N. *Tetrahedron* **1974**, *30,* 3525.

S0002-7863(97)02411-6 CCC: $14.00

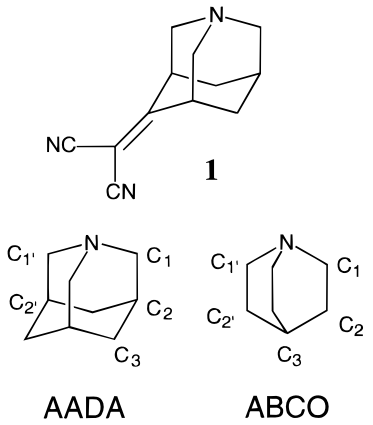

Figure 1. Structures and atom numbering of (a) dicyanoethylene−azaadamantane (**1**), (b) 1-azabicyclo[2.2.2]octane (ABCO), and (c) 1-azaadamantane (AADA).

and vibrational frequencies occurring upon ionization or, more generally, comparison of the geometric and vibrational properties of the ground state of the radical cation with those of the ground state of the neutral molecule. Experimental studies along these lines would most naturally proceed by employing photoelectron spectroscopy, which enables such a direct comparison to be made. The spectral resolution, which can be obtained with photoelectron spectroscopy, is normally, however, limited to about 100 cm^{-1}. It would consequently be much preferred if the same information could be extracted by studies on specific excited states of the neutral molecule, since such studies can be performed by employing high-resolution techniques such as fluorescence excitation spectroscopy with lasers. Rydberg states converging upon the lowest ionic state are excellent candidates in this respect, since their geometry and vibrational properties can be expected to be very similar to those of their ionic core.[11] This being the case, calculations on the ground state of the radical cation allow one to learn about this species itself, but also to obtain a useful approximation to the structure and force field of the Rydberg states. An additional advantage is that such calculations are in general much easier to perform than calculations on excited states of the neutral molecule.

In the present work we try and successfully combine the merits of both the experimental and the theoretical approach in a study of the electron donor building block of **1**, 1-azaadamantane (AADA), and, for comparison, 1-aza[2.2.2]bicyclooctane (ABCO). Experimentally, one-photon fluorescence excitation spectroscopy and dispersed emission spectroscopy are performed on the lowest excited singlet state (S_1) of the neutral molecules seeded in a supersonic jet expansion. This state is the [1 $^2A_1$]3s Rydberg state for both molecules and thus fulfills the criteria set above. Theoretically, the initial analysis of the spectral data rests on quantum-chemical calculations. Density functional calculations have emerged as an economic and accurate approach to molecular calculations, and are very appropriate for molecules of this size.[12−15] Equilibrium geometries and vibrational force fields are calculated for the ground state of the neutral molecule (S_0) and of the radical cation (D_0). The vibrational frequencies are compared with experimental values to validate the calculations. The computed data allow a good prediction of intensity patterns in excitation and emission spectra, while subsequent refinement of the excited state equilibrium geometries by using the experimental intensities serves to investigate the difference in structure between the "real" excited states and the model radical cations. The geometry changes, expressed in mode-specific reorganization energies, emerging from these experimental and theoretical analyses will be compared for the AADA/AADA$^{\bullet+}$ system with the values obtained from the resonance Raman study of **1**.[7] Apart from enabling an elegant comparison between the properties of S_0, S_1, and D_0, the combination of experiment and theory also elucidates the finer details of the vibronic wave functions of S_1. For both molecules non-totally symmetric vibrational bands are observed in the fluorescence excitation spectra, indicative of vibronic coupling with higher-lying states.

II. Experimental and Theoretical Details

A. Experimental Procedures. The experimental setup for performing fluorescence excitation spectroscopy on samples seeded in a continuous supersonic jet has been described in detail elsewhere.[16,17] Briefly, excitation was performed by using a XeCl excimer laser (Lambda Physik EMG103MSC) working at a repetition rate of 60 Hz, which pumped a dye laser (Lumonics HyperDye-300) operating on Coumarine 500, Coumarine 480, or Coumarine 460. The output of this dye laser was frequency-doubled by using an angle-tuned BBO crystal in an Inrad Autotracker II unit. The resulting excitation light had a spectral band width of about 0.15 cm^{-1} and a pulse duration of about 15 ns. Calibration of the wavelength of the dye laser output was achieved by using the optogalvanic spectrum of Ne excited in a hollow-cathode discharge. The intensity of the frequency-doubled dye laser light was monitored by measuring the intensity of a reflection with an EG&G radiometer model 580, which was read out by a computer controlling the experiment.

This excitation beam was steered into the vacuum chamber, where it crossed at right angles a continuous free jet made by expanding 3 bar of He seeded with ABCO or AADA room temperature vapor through a nozzle with a diameter of 100 μm into a vacuum chamber pumped by an Edwards Roots pump (EH500, 500 m^3/h), backed by a rotary forepump (Edwards E2M80, 80 m^3/h). Excitation of the jet occurred at a distance of 10 nozzle diameters, *i.e.*, 1 mm, from the nozzle. The fluorescence from the jet-cooled compounds was collected at right angles with respect to the excitation light and the molecular beam by a spherical quartz condenser (Melles Griot 01MCP119, diameter 50 mm, focal length 50 mm) and imaged onto the slit of a Zeiss M20 grating monochromator equipped with an EMI 9558 QA (S20) photomultiplier.

In the fluorescence excitation experiments the monochromator was used in second order with a slit width of 5 mm, resulting in a spectral resolution of 12.5 nm. For ABCO and AADA, center emission wavelengths of 543 (271.5 in second order) and 575 (287.5) nm, respectively, were used. The output of the photomultiplier was integrated during 1 μs with a boxcar integrator (SR250), whose output was read out and averaged by the computer. In a typical experiment, excitation spectra were obtained by scanning the dye laser in steps of 0.1 cm^{-1}, averaging over 10 laser pulses, and dividing the fluorescence signal by the laser intensity as measured by the radiometer.

For some of the relevant bands observed in the excitation spectra single level emission spectra have been recorded. In these experiments the photomultiplier was cooled (−78 °C) with a mixture of ethanol and dry ice to reduce the dark current. Emission spectra were obtained by scanning the monochromator with a slit width of 0.02 mm, resulting in a resolution of about 14 cm^{-1}, and averaging the signal over 60 laser pulses.

Apart from fluorescence excitation experiments, from which the vibrational frequencies in the excited state were obtained, Raman spectra have also been measured for both compounds to determine such frequencies in their ground states. FT-Raman spectra with a resolution of 4 cm^{-1} have been obtained with use of a Bruker RFS 100 employing a Nd-YAG laser giving 400 mW at 1064 nm.

(11) Herzberg, G. *Molecular Spectra and Molecular Structure, Vol. III. Electronic Spectra and Electronic Structure of Polyatomic Molecules*; Van Nostrand: New York, 1966.
(12) Johnson, B. G.; Gill, P. M. W.; Pople, J. A. *J. Chem. Phys.* **1993**, *98*, 5612.
(13) Eriksson, L. A.; Lunell, S.; Boyd, R. J. *J. Am. Chem. Soc.* **1993**, *115*, 6896.
(14) St. Amant, A.; Cornell, W. D.; Kollmann, P. A.; Halgren, T. A. *J. Comput. Chem.* **1995**, *16*, 1483.
(15) Brouwer, A. M. *J. Phys. Chem. A* **1997**, *101*, 3626.
(16) Wegewijs, B. R. Ph.D. Thesis, University of Amsterdam, 1994.
(17) Pérez-Salgado, P. Ph.D. Thesis, University of Amsterdam, 1992.

ABCO was obtained from Aldrich and was used without further purification. AADA was synthesized by Wolff-Kishner reduction of 1-azaadamantanone.[18]

B. Theoretical Procedures. Calculations on the ground states of the neutral molecule and of the radical cation of ABCO and AADA were performed with the Gaussian 94 program.[19] Optimized geometries and harmonic force fields were obtained by using density functional theory ((U)B3LYP).[20] Several types of basis sets have been employed in these calculations. Although the differences in vibrational frequencies between these calculations with different basis sets were found to be minimal, the vibrational overlap integrals were observed to be more dependent on the quality of the basis set. In this respect the 6-311G* basis set gave the best agreement between experiment and theory, and those results will therefore be discussed.

A number of calculations have also been performed on the lowest excited singlet state of the neutral molecule. In these calculations, performed with the GAMESS-DAKOTA package,[21] GVB and CASSCF methods have been applied in combination with the Dunning/Hay (9s 5p|3s)/[3s 2p|2s] "double-ζ" basis set[22] augmented with a split Rydberg 3s orbital on the carbon atoms (exponents 0.0437 and 0.01725) and the nitrogen atom (exponents 0.0532 and 0.021).[22]

The intensities of vibronic transitions observed in our excitation spectra were simulated by using the Condon approximation, in which the intensity of a vibronic transition is directly proportional to the square of the relevant vibrational overlap integral, *i.e.*, it assumes that the electronic transition moment is independent of the nuclear geometry. Vibrational overlap integrals were calculated by employing the theory as developed by Doktorov *et al.*,[23] using the experimental frequencies as determined from the present study.

III. Results and Discussion

In this section we will first be concerned with the results of our experimental and theoretical studies on the S_0, S_1, and D_0 states of ABCO, since the spectroscopy of this molecule has been studied more extensively[24−34] than the spectroscopy of AADA.[10,27,35] From the analysis of excitation and single level emission spectra of the S_1 state of ABCO it will become clear that some of the previously proposed[34] assignments of bands in the $S_1 \leftarrow S_0$ spectrum need to revised, while at the same time the role of vibronic coupling is highlighted. The applied approach being validated by the results obtained for ABCO, it will subsequently be used to study AADA. The results of these studies will be compared with those on ABCO and employed to study the mode-specific reorganization energies associated with the donor part in the electron-donor−acceptor system **1**.

A. Azabicyclo[2.2.2]octane. The one-photon fluorescence excitation spectrum of the $S_1(2\ ^1A_1) \leftarrow S_0(1\ ^1A_1)$ transition of ABCO seeded in a supersonic jet expansion of He as obtained in the present study is shown in Figure 2a. This spectrum was constructed by linking consecutive scans over shorter wavelength ranges and linearly scaling the intensities from one scan with respect to the other, using bands which were present in both scans. The spectrum is in good agreement with the previously reported jet-cooled spectrum of Fujii *et al.*,[34] although we find the 0−0 transition at 39 092 cm^{-1}, somewhat different from their value of 39 095 cm^{-1}. Moreover, Figure 2a shows that in the region above 41 900 cm^{-1}, which was not reported previously, vibrational structure can still be observed. Similar to all the other transitions observed roughly up to 2500 cm^{-1} from the 0−0 transition, the 0−0 transition exhibits rotational structure in the form of an intense, narrow (fwhm 0.3 cm^{-1}) Q branch and broader, although weaker, P and R branches (see the inset in Figure 2a). At energies larger than *ca.* 2500 cm^{-1} above the 0−0 transition the vibrational structure becomes very congested, and bands start to broaden.

The $S_1 \leftarrow S_0$ excitation spectrum exhibits a considerable amount of vibrational activity, indicating that the geometry of the molecule is changed significantly upon excitation. Similar to other saturated amines, these geometry changes can be explained as resulting from the change in the hybridization of the nitrogen atom upon excitation of a lone-pair electron. In the experimental excitation spectrum this change in geometry comes most prominently forward in the activities of the vibrations with frequencies of 626, 774, and 922 cm^{-1}, whose overtones and combination bands determine the dominant features of the excitation spectrum. Previously, these frequencies have been assigned to the $\nu_{12}(a_1)$ (cage squashing mode), $\nu_{11}(a_1)$, and $\nu_9(a_1)$ modes, respectively.[30,34] Apart from these modes, considerable activity is also observed in the modes at 937, 1240, and 1263 cm^{-1}, which have tentatively been assigned to the $\nu_{33}(e)$, $\nu_{31}(e)$, and $\nu_{29}(e)$ modes, respectively.[34] To put such assignments on a firmer basis and to explain the finer details of the excitation spectrum it is clear, however, that high-quality ab initio calculations are most welcome.

Ab initio calculations of the geometry of the ground state of ABCO at the B3LYP/6-311G* level lead to the geometrical parameters reported in Table 1. The experimental structure of ABCO in the gas phase has been investigated by using rotational spectroscopy[36] and electron diffraction.[37] The results from the detailed microwave study of Hirota and Suenaga[36] are most consistent with the experimentally determined structure of the closely related diamine 1,4-diazabicyclo[2.2.2]octane (DABCO). The B3LYP method in general performs well in the prediction of molecular structures,[12−15] and the structures predicted for ABCO as well as for DABCO[38] agree very well with experiment. The harmonic force field calculated at this geometry gives rise to the frequencies reported in Table 2. A good agreement is found between the calculated vibrational frequencies and those determined from previous[39] IR and present FT-Raman spectra. The B3LYP computed frequencies are systematically greater than the experimental ones. As was recently shown,[40,41] simple

(18) Becker, D. P.; Flynn, D. L. *Synthesis* **1992**, 1080.
(19) Gaussian 94, Frisch, M. J.; Trucks, G. W.; Schlegel, H. B.; Gill, P. M. W.; Johnson, B. G.; Robb, M. A.; Cheeseman, J. R.; Keith, T.; Petersson, G. A.; Montgomery, J. A.; Raghavachari, K.; Al-Laham, M. A.; Zakrzewski, V. G.; Ortiz, J. V.; Foresman, J. B.; Cioslowski, J.; Stefanov, B. B.; Nanayakkara, A.; Challacombe, M.; Peng, C. Y.; Ayala, P. Y.; Chen, W.; Wong, M. W.; Andres, J. L.; Reprogle, E. S.; Gomperts, R.; Martin, R. L.; Fox, D. J.; Binkley, J. S.; Defrees, D. J.; Baker, J.; Stewart, J. J. P.; Head-Gordon, M.; Gonzales, C.; Pople, J. A.; Pittsburgh: PA, 1995.
(20) Becke, A. D. *J. Chem. Phys.* **1993**, *98*, 5648.
(21) Schmidt, M. W.; Baldridge, K. K.; Boatz, J. A.; Koseki, S.; Gordon, M. S.; Nguyen, K. A.; Windus, T. L.; Elbert, S. T. *QCPE Bull.* **1990**, *10*, 52.
(22) Dunning, T. H.; Hay, P. J. In *Methods of Electronic structure theory;* Schaefer, H. F., Ed.; Plenum Press: New York, 1977; Vol. 1.
(23) Doktorov, E. V.; Malkin, I. A.; Man'ko, V. I. *J. Mol. Spectrosc.* **1977**, *64*, 302.
(24) Halpern, A. M.; Roebber, J. L.; Weiss, K. *J. Chem. Phys.* **1968**, *49*, 1348.
(25) Halpern, A. M. *J. Am. Chem. Soc.* **1974**, *96*, 4392.
(26) Halpern, A. M. *J. Am. Chem. Soc.* **1974**, *96*, 7655.
(27) Halpern, A. M.; Ravinet, P.; Sternfels, R. J. *J. Am. Chem. Soc.* **1977**, *99*, 169.
(28) Parker, D. H.; Avouris, P. *Chem. Phys. Lett.* **1978**, *53*, 515.
(29) Halpern, A. M.; Gerrity, D. P.; Rothberg, L. J.; Vaida, V. *J. Chem. Phys.* **1982**, *76*, 102.
(30) Gonohe, N.; Yatsuda, N.; Mikami, N.; Ito, M. *Bull. Chem. Soc. Jpn.* **1982**, *55*, 2796.
(31) Kuno, H.; Kasatani, K.; Kawasaki, M.; Sato, H. *Bull. Chem. Soc. Jpn.* **1982**, *55*, 3097.
(32) Fisanick, G. J.; Eichelberger, T. S.; Robin, M. B.; Kuebler, N. A. *J. Phys. Chem.* **1983**, *87*, 2240.
(33) Weber, A. M.; Acharya, A.; Parker, D. H. *J. Phys. Chem.* **1984**, *88*, 6087.
(34) Fujii, M.; Mikami, N.; Ito, M. *Chem. Phys.* **1985**, *99*, 193.
(35) Halpern, A. M. *Mol. Photochem.* **1973**, *5*, 517.
(36) Hirota, E.; Suenaga, S. *J. Mol. Spectrosc.* **1972**, *42*, 127.
(37) Schei, H.; Shen, Q.; Hilderbrandt, R. L. *J. Mol. Struct.* **1980**, *65*, 297.
(38) Zwier, J. M.; Brouwer, A. M.; Buma, W. J. Submitted for publication.
(39) Brüesch, P. *Spectrochim. Acta* **1966**, *22*, 861.

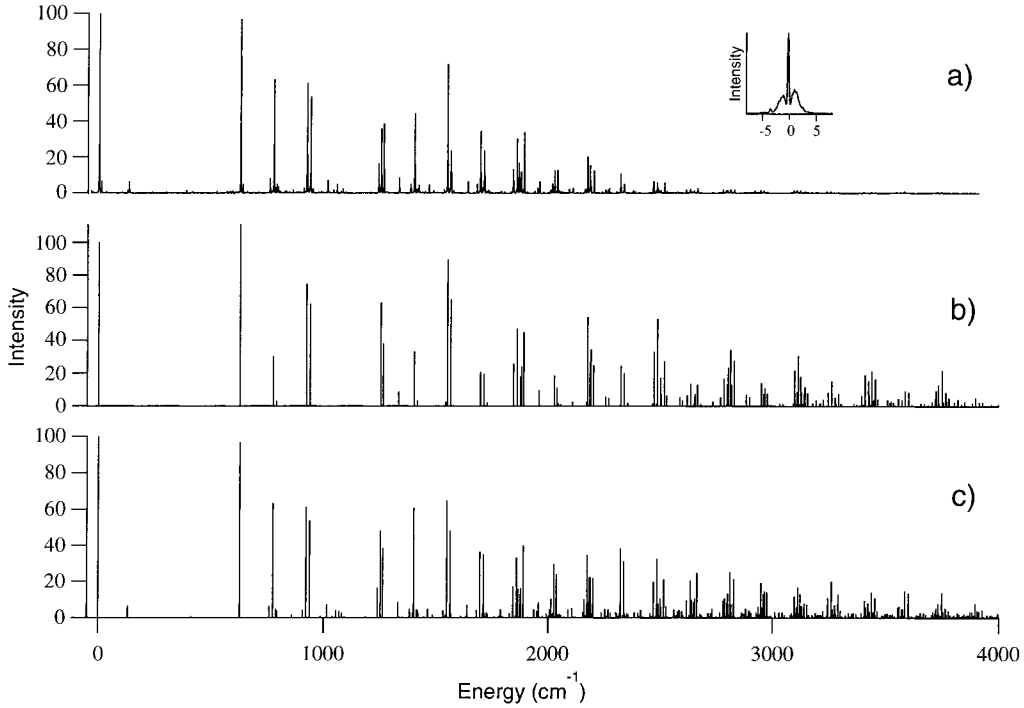

Figure 2. Excitation spectrum of the $S_1 \leftarrow S_0$ transition of 1-azabicyclo[2.2.2]octane. The excitation energy is given with respect to the energy of the 0−0 transition located at 39 092 cm^{-1}. (a) Experimentally observed fluorescence excitation spectrum. (b) Spectrum predicted by employing Franck−Condon factors for transitions from the zero-point level in S_0 to a_1 levels in S_1, and which have been calculated from the B3LYP/6-311G* equilibrium geometries and force fields of S_0 and D_0. (c) Spectrum predicted by employing the equilibrium geometry of S_1 as it was reconstructed from the experimentally observed intensities of the $\nu_i(a_1)^1{}_0$ transitions. This spectrum also contains, apart from transitions to a_1 levels, transitions to e levels (see text).

Table 1. Selected Geometrical Parameters (Å and deg) of the Equilibrium Geometries Calculated at the B3LYP/6-311G* Level for the $S_0(1\ ^1A_1)$ Ground State of Neutral ABCO and the $D_0(1\ ^2A_1)$ Ground State of the Radical Cation[a]

	$S_0(1\ ^1A_1)$[b]	$S_0(1\ ^1A_1)$[c]	$D_0(1\ ^2A_1)$	$S_1(2\ ^1A_1)$
$N-C_1$	1.472	1.472	−0.024	−0.034
C_1-C_2	1.562	1.562	0.036	0.038
C_2-C_3	1.541	1.541	−0.005	0.001
C_1-H_1	1.094	1.09	−0.005	0.000
C_2-H_2	1.095	1.09	−0.004	0.000
C_3-H_3	1.094	1.09	0.001	0.000
$C_1NC_{1'}$	109.3	110.5	5.3	5.3
NC_1H_1	107.8	109.3	1.7	1.7
NC_1C_2	111.8	110.0	−6.8	−6.3
$C_1C_2H_2$	111.1	109.6	−2.3	−2.4
$C_1C_2C_3$	108.0	109.0	0.1	0.1
$C_2C_3H_3$	110.2	110.6	−0.7	−0.2
$C_2C_3C_{2'}$	108.7	108.0	0.7	0.2

[a] The parameters as reported for the geometry of the lowest excited singlet state of the neutral molecule have been obtained by employing observed intensities of the $\nu_i(a_1)^1{}_0$ transitions in the $S_1 \leftarrow S_0$ excitation spectrum. Parameters given for D_0 and S_1 are given as changes with respect to the geometry of S_0. [b] Computed, this work. [c] Experimental, ref 36.

linear scaling of the computed frequencies by a factor of 0.961 is usually sufficient to achieve a good agreement. In this case the optimal scaling factor is 0.975, which leads to a root mean square deviation of experimental and scaled frequencies of 13 cm^{-1}, with a largest absolute error of 23 cm^{-1}. Closer inspection, however, reveals that in this case the low-frequency vibrations are too low after scaling, so that the uniform scaling procedure is not quite appropriate in the case of ABCO.

Calculations on the first excited state of ABCO at a similar level prove to be considerably more difficult. Previous CI[42,43] and CASSCF[44] studies concentrated primarily on the vertical excitation energies and character of the lower excited states, and did not consider the excited state force fields. Our initial attempts to obtain the harmonic force field of S_1 at the CASSCF level were not successful due to convergence problems of the CASSCF wave function. At the GVB/ROHF level such a force field could be obtained, but this force field was not judged to be adequate since it did not lead to accurate predictions of the vibrational intensities in the $S_1 \leftarrow S_0$ excitation spectrum (*vide infra*).

The lowest excited singlet state of ABCO derives from the excitation of a lone pair electron to a Rydberg orbital, which contains a dominant contribution from the 3s orbital on the nitrogen atom.[42,44] In such a description the state can be envisaged as an ionic core, the $1\ ^2A_1$ ground state D_0 of the radical cation, to which a Rydberg electron is loosely bound. The equilibrium geometry and vibrational properties of the lowest excited singlet state are therefore expected to resemble to a large extent, if not completely, those of the $1\ ^2A_1$ ionic core, *i.e.*, in principle the $S_1 \leftarrow S_0$ excitation spectrum might be modeled by using the equilibrium geometries and harmonic force fields of S_0 and D_0.

The equilibrium geometry obtained for the ground state of the radical cation at the UB3LYP/6-311G* level is given in Table 1. In this state the apex angle $C_1NC_{1'}$ has been changed from a pure sp^3 angle of 109.3° in the ground state of the neutral molecule to 114.6°. A similar change was found in the CASSCF calculations on the S_1 state.[44] Simultaneously, the $N-C_1$ bond length decreases by 0.02 Å, while the C_1-C_2 bond length increases by 0.04 Å. These changes reveal the change from a purely sp^3-hybridized to a more sp^2-hybridized nitrogen atom. The vibrational frequencies calculated for the ground state of the radical cation are given in Table 2.

(40) Rauhut, G.; Pulay, P. *J. Phys. Chem.* **1995**, *99*, 3093.
(41) Scott, A. P.; Radom, L. *J. Phys. Chem.* **1996**, *100*, 16502.
(42) Avouris, P.; Rossi, A. R. *J. Phys. Chem.* **1981**, *85*, 2340.
(43) Galasso, V. *Chem. Phys.* **1997**, *215*, 183.
(44) Disselkamp, R.; Shang, Q.-Y.; Bernstein, E. R. *J. Phys. Chem.* **1995**, *99*, 7227.

Table 2. Experimental and Calculated (B3LYP/6-311G*) Fundamental Vibrational Frequencies (cm^{-1}) of a_1 and e Vibrations of ABCO in the Ground and First Excited States and Intensities in the $S_1 \leftarrow S_0$ Excitation Spectrum[a]

		vibrational frequencies				intensities	
		S_0(exp)	S_0(calc)	S_1(exp)	D_0(calc)	I(exp)	I(calc)[b]
a_1	ν_{12}	601	610	626.1	637.4	97	111
	ν_{11}	777	785	774.3	782.2	63	30
	ν_{10}	801	800	789.0	790.0	5	3
	ν_9	970	971	922.0	932.0	61	75
	ν_8	1001	1019	937.3	947.8	54	62
	ν_7	1328	1358	1263.2	1320.2	39	38
	ν_6	1350	1392	1332.3	1377.0	9	9
	ν_5	1459	1509	1463.7[c]	1519.8	5[f]	0
	ν_4	1471	1529	1541.3[d]	1560.1	2[f]	3
e	ν_{38}	304	295		298.8		
	ν_{37}	405	405	413.3	420.8	1	
	ν_{36}	542	550		503.4		
	ν_{35}	823	830	793.9	801.2	4	
	ν_{34}	877	879	859.4	853.9	2	
	ν_{33}	993	1002	985.9	987.8	1	
	ν_{32}	1054	1069	1014.4	1024.3	7	
	ν_{31}	1114	1142	1080.5	1124.2	3	
	ν_{30}	1202	1234	1092.8	1191.5	1	
	ν_{29}	1271	1307	1239.8	1265.8	17	
	ν_{28}	1300	1348	1324.5[e]	1330.0	<1	
	ν_{27}	1318	1364	1324.5[e]	1338.5	<1	
	ν_{26}	1342	1383	1381.5	1384.4	5	
	ν_{25}	1443	1497	1447.1[c]	1493.6	1	
	ν_{24}		1512	1463.7[c]	1518.1	5	

[a] Intensities are given relative to the intensity of the 0−0 transition, which is taken as 100. [b] Calculated by using equilibrium geometry and the force field of the ground state radical cation. [c] The band at 1463.7 cm^{-1} from the 0−0 transition can be attributed to the 5^1_0, 25^1_0, or 24^1_0 transition. [d] In this region the 1538.0, 1541.3, or 1542.3 cm^{-1} band corresponds to the 4^1_0 transition. [e] The very weak band at 1324.5 cm^{-1} can be attributed to either the 28^1_0 or the 27^1_0 transition. [f] Intensity not employed in the reconstruction of the excited state equilibrium geometry from observed $\nu_i(a_1)^1_0$ experimental intensities.

Under the assumption that the equilibrium geometry and harmonic force field of the lowest excited singlet state can be taken as those of the ground state of the radical cation, one can now attempt to assign the vibrational bands observed in the experimental $S_1 \leftarrow S_0$ excitation spectrum. Such assignments have been performed guided by three considerations. First, comparison of calculated and experimental frequencies for the ground state of the neutral molecule (see Table 2) shows that the calculated frequencies are too high by 0−4%. Similar deviations are to be expected for the vibrational frequencies calculated for the ground state of the radical cation. Secondly, within the Condon approximation only transitions to totally symmetric vibrational levels of the lowest excited singlet state are possible since in our supersonic beam experiments excitation occurs predominantly from the vibrational ground state. It is important to notice that the assignment of bands to levels of e symmetry, as has been proposed previously, implies a breakdown of the Condon approximation, for example by vibronic coupling with higher electronically excited states of E symmetry. While vibronic coupling is in principle possible, and indeed turns out to be of importance (*vide infra*), we have first tried to assign bands to transitions to totally symmetric levels. Thirdly, experimentally observed vibrational intensities have been compared with predicted intensities for transitions to levels of a_1 symmetry calculated from overlap integrals between the vibrational wave functions of ground and excited state. The $S_1 \leftarrow S_0$ excitation spectrum predicted in this way is depicted in Figure 2b.

Spectra a and b in Figure 2 show a remarkable agreement, apart from differences in peak intensities of bands above *ca.* 2500 cm^{-1}, which is in part due to the broadening of the bands at higher energies. Indeed, the comparison of the two spectra leads to a straightforward assignment of the majority of the observed bands as fundamentals, overtones, and combination bands of a_1 vibrations and combinations with the first overtone of the low-frequency torsional vibration $\nu_{19}(a_2)$ located at 132.7 cm^{-1}. From the frequencies of the overtones and combination bands it can be concluded that the potential energy surface of the excited state is to a good approximation harmonic.

At the same time, however, it becomes apparent that a number of bands cannot be accounted for. Examples include the band at 793.9 cm^{-1}, bands in the region between 1000 and 1100 cm^{-1}, and the band at 1239.8 cm^{-1}. Calculated frequencies for the radical cation lead to the conclusion that these transitions should be attributed to $\nu_i(e)^1_0$ vibrations and their combinations with a_1 vibrations. The assignment of bands to vibrational levels of a_1 symmetry was led and corroborated by the theoretical prediction of their intensities. Such predictions are considerably more difficult for transitions to levels of e symmetry, since they obtain their transition moment from vibronic coupling. One might hope that the two types of transitions can be distinguished on account of a different rotational contour, since transitions to a_1 and e levels will exhibit parallel and perpendicular bands, respectively. However, as the rotational constants of the molecule show an almost spherical symmetry in both the ground and excited states, both types of bands are expected to be similar. Despite these limitations, identification of the e vibrations follows straightforwardly from the comparison between computed and experimental frequencies.

The frequencies of the identified a_1 and e vibrations are given in Table 2, together with their experimental intensities and the intensities predicted for the transitions to the a_1 fundamentals. The excitation spectrum allows an unambiguous identification of the frequencies of the a_1 vibrations in the excited state, with the exception of ν_5 and ν_4. The 5^1_0 transition is in an energy region where the $25(e)^1_0$ and $24(e)^1_0$ transitions are also expected. Since the 5^1_0 transition is predicted to have a low intensity, and the observed intensity (5%) is not at odds with a vibronically induced intensity for an e vibration, it is not possible to assign the band at 1463.7 cm^{-1} above the 0−0 transition unambiguously to either one of these three possibilities. The transition to the fundamental of ν_4 is expected to be located close to the strong $12^1_0 9^1_0$ (1546.5 cm^{-1}) band. Here three bands with about equal intensities are observed at 1538.0, 1541.3, and 1542.3 cm^{-1}. Although our analysis makes it clear that one of these three bands should correspond to the 4^1_0 transition, it is not possible to make a definite assignment. With respect to the e vibrations, we stress that the assignments of ν_{30}, ν_{28}, ν_{27}, ν_{25}, and ν_{24} are more tentative. The weak band at 1092.8 cm^{-1} cannot be assigned to a transition to an a_1 level, but its assignment as 30^1_0 implies a scaling factor of 0.917, which falls outside the range observed for the other vibrations. Assignment of the 28^1_0 and 27^1_0 transitions is hindered by the fact that these two vibrations are predicted to have similar frequencies. Analogous problems arise in assigning the 25^1_0 and 24^1_0 transitions, which, moreover, are located near the expected 5^1_0 transition. Using the frequencies reported in Table 2 and ignoring the band at 1092.8 cm^{-1}, we come to the conclusion that the computed frequencies are again too high by 0−4%. The usual linear scaling procedure in this case gives a root-mean-square error of 17 cm^{-1}, and a largest absolute error of 31 cm^{-1}. The agreement is very good, although somewhat poorer than usual, which may reflect the fact that we compare the experimental data for the excited state with computed data of the radical cation.

In the present study the bands at 937.3 and 1263.2 cm^{-1} have been assigned to the 8^1_0 and 7^1_0 transitions, while previously

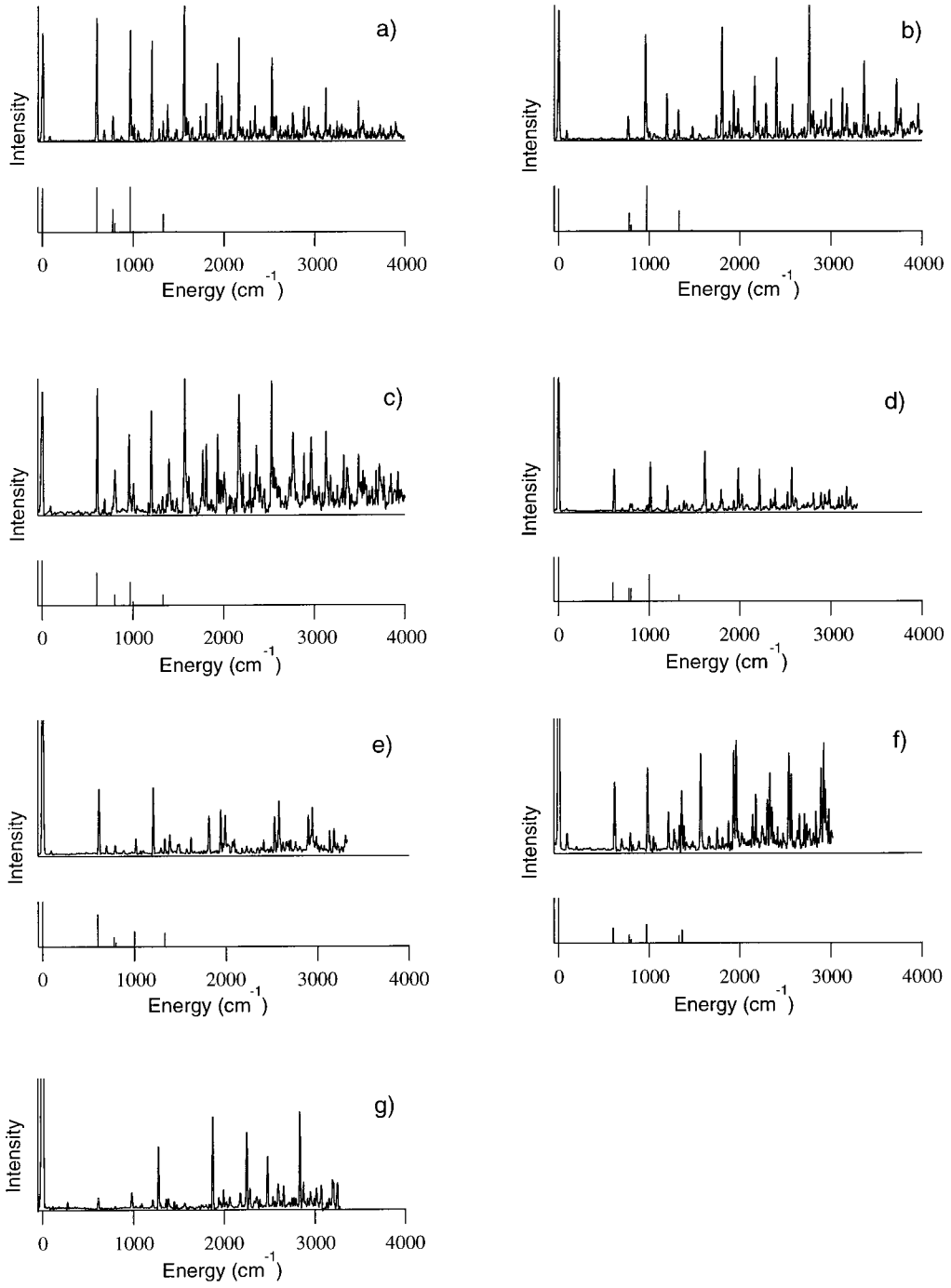

Figure 3. Single level emission spectra from selected levels in the lowest excited state of ABCO. Fluorescence wavelengths are given as shifts from the excitation wavelength. Below spectra a−f a stick spectrum is included representing the intensities of the transitions to $\nu_i(a_1)_1$ levels in the ground state predicted by Franck−Condon calculations employing the B3LYP/6-311G* equilibrium geometries and force fields of S_0 and D_0: (a) 0^0 level, (b) 12^1 (a_1) level, (c) 11^1 (a_1) level, (d) 9^1 (a_1) level, (e) 8^1 (a_1) level, (f) 7^1 (a_1) level, and (g) 29^1 (e) level.

assignments to e levels were proposed.[34] Single level emission spectra recorded for these bands and a number of other strong bands fully support the present assignments. Spectra a−g in Figure 3 display such spectra for emission from the 0^0, 12^1, 11^1, 9^1, 8^1, 7^1, and 29^1 levels. Stick spectra below parts a−f in Figure 3 indicate the Franck−Condon factors calculated for emission from these levels to $\nu_i(a_1) = 1$ levels in the ground state. In general, experimentally observed and theoretically predicted intensities agree well, buttressing our assignments for these bands. While in Figure 3a−f dominant activity is found in transitions to a_1 ground state levels, Figure 3g shows that emission from the 29^1 level occurs with an intensity distribution as observed for emission from the 0^0 level, but displaced by one quantum of the ν_{29} vibration in the ground state (1271 cm^{-1}). This is in perfect agreement with *a priori* expectations for emission from an e level in the excited state.

The activity of e vibrations in the excitation spectrum shows that the lowest excited singlet state is subject to vibronic coupling to states of E symmetry, most probably the $3p_{x,y}(1\,^1E)$ Rydberg state located at 43 750 cm^{-1}.[33,45] Experimental[24,45] and theoretical[42,43,45] studies indicate that the oscillator strength of the transition to this state is about one order of magnitude larger than that of the transition to the lowest excited singlet state. Because of this large difference even a relatively weak coupling of the two states will show up prominently in the excitation spectrum to the lowest excited singlet state. The

(45) Zwier, J. M.; Brouwer, A. M.; Buma, W. J. To be submitted for publication.

Table 3. Duschinsky Matrix for the a_1 Vibrations in ABCO Calculated from the Force Fields of the Ground State of the Neutral Molecule and the Radical Cation[a]

	D_0								
S_0	ν_{12}	ν_{11}	ν_{10}	ν_9	ν_8	ν_7	ν_6	ν_5	ν_4
ν_{12}	**0.983**	−0.048	0.031	0.135	−0.100	−0.044	0.001	0.008	−0.014
ν_{11}	−0.054	**−0.493**	**0.866**	−0.023	−0.065	0.021	0.010	−0.003	0.016
ν_{10}	0.054	**0.852**	**0.485**	−0.186	0.013	0.010	0.001	−0.009	−0.007
ν_9	−0.034	0.088	0.116	**0.741**	**0.652**	0.015	0.057	0.002	−0.022
ν_8	0.148	−0.139	−0.026	**−0.619**	**0.741**	−0.154	−0.044	0.004	−0.012
ν_7	0.061	−0.023	−0.032	−0.121	0.083	**0.809**	**0.560**	0.043	0.046
ν_6	−0.034	0.006	0.003	−0.002	−0.063	**−0.554**	**0.817**	0.076	−0.120
ν_5	−0.011	−0.001	0.009	−0.004	−0.008	0.058	−0.111	**0.876**	**−0.466**
ν_4	0.004	0.016	−0.002	0.015	0.010	−0.090	0.024	**0.475**	**0.875**

[a] Dominant contributions are given in bold.

observation of the role of vibronic coupling with the $3p_{x,y}$ Rydberg state raises the question whether vibronic coupling *via* a_1 vibrations with the $3p_z(3\ ^1A_1)$ Rydberg state located at 44 390 cm^{-1} [33,45] might similarly influence the transition intensities to a_1 vibrational levels. A quantitative analysis would obviously require knowledge of the relevant vibronic coupling matrix elements, but the experimental[33,45] and theoretical[42,45] conclusion that the oscillator strengths of the transitions to the $3p_z$ and $3p_{x,y}$ Rydberg states are in the ratio of about 1:3 indicates that the influence of interaction with the $3p_z$ Rydberg state cannot *a priori* be excluded.

As yet, the activities of the various a_1 vibrations in the $S_1 \leftarrow S_0$ excitation spectrum have been taken as evidence for geometry changes occurring upon excitation. The Duschinsky matrix calculated for the a_1 vibrations and given in Table 3 shows that apart from geometry changes considerable mode scrambling also occurs. In fact, the only vibration that retains its original ground state character upon excitation is the "cage squashing" mode ν_{12}. Model calculations, in which the Duschinsky matrix is taken as the unit matrix, demonstrate that the calculated intensities vary considerably with the amount of mode scrambling, although the qualitative features of the excitation spectrum remain unchanged. It should consequently be concluded that the quantitative activities of the a_1 vibrations are determined not only by differences in ground and excited state geometry but also by normal mode rotations occurring upon excitation.

Despite the impressive agreement between the experimentally obtained and theoretically predicted $S_1 \leftarrow S_0$ excitation spectrum, some minor differences between the two spectra remain. As discussed above, these differences might be explained by vibronic coupling with the $3p_z$ Rydberg state, but they might also be related to small differences between the equilibrium geometries and force fields of the lowest excited singlet state and the ground state of the radical cation that we used as a model. A complete unraveling of the relative importance of these three factors is not within reach on the basis of the present measurements and calculations. It is nevertheless of interest to see what equilibrium geometry of the excited state would be implied if the differences between experiment and theory would be completely attributed to differences in the equilibrium geometry of S_1 and D_0. To this purpose we assume that the equilibrium geometry of S_0 and the force fields of S_0 and S_1 are calculated "exactly", and we reconstruct the equilibrium geometry of the lowest excited singlet state from the experimentally observed intensities of the $\nu_i(a_1)^1_0$ transitions,[23] except those of the 5^1_0 and 4^1_0 transitions, which could not be identified completely unambiguously (*vide supra*). In this reconstruction the signs of the normal mode displacements—which are in principle arbitrary, since the experimentally observed intensities are proportional to the square of the vibrational overlap integrals—were taken equal to the signs of the displacements calculated with the equilibrium geometry of the ground state of the radical cation. The resulting geometrical parameters are given in Table 1, which shows that the difference between the experimentally observed and ab initio computed intensities of the $\nu_i(a_1)^1_0$ transitions corresponds with only minor geometrical differences between S_1 and D_0.

The $S_1 \leftarrow S_0$ excitation spectrum calculated by using the "experimentally" determined equilibrium geometry of the lowest excited singlet state is depicted in Figure 2c. In this spectrum transitions to levels of e symmetry are also incorporated. The intensity of $\nu_i(e)^1_0$ transitions was taken as the experimentally observed intensity, while the intensities of combination bands with a_1 levels were calculated as the product of the predicted transition intensity to that particular a_1 level and the experimentally observed transition intensity to the fundamental of the e vibration. In a similar way intensities have been calculated for transitions to combination bands based upon the 19^2_0 transition, whose intensity was taken as determined experimentally. Comparison with the experimental spectrum shows that the intensities of many of the overtones and combination bands are predicted somewhat better than in the original approximation (Figure 2b). It thus would seem that the equilibrium geometries of S_1 and D_0 are not exactly the same, although the absolute differences are small.

B. 1-Azaadamantane. The one-photon fluorescence excitation spectrum of the $S_1(2\ ^1A_1) \leftarrow S_0(1\ ^1A_1)$ transition of AADA seeded in a supersonic jet expansion of He is depicted in Figure 4a. The origin of the transition is found at 37 725 cm^{-1}, which is significantly different from a previously reported value of 37 664 cm^{-1}.[27] It is not clear why there is such a large difference between the two values, also because in the latter publication the excitation spectra were not shown. The bands in the excitation spectrum display a similar rotational contour as observed for ABCO: a strong, narrow (0.3 cm^{-1}) Q branch accompanied by weaker and broader P and R branches (see the inset in Figure 4a). While in ABCO bands seemed to become broader at excitation energies above *ca.* 2500 cm^{-1}, broadening in the excitation spectrum of AADA is considerably less apparent: up until the last recorded band around 3400 cm^{-1} the rotational contour observed for the 0−0 transition remains visible. On the basis of the width of the P and R branches it can be concluded that similar rotational temperatures are reached in the supersonic expansion for ABCO and AADA. The larger number of hot bands in the excitation spectrum of AADA indicates, on the other hand, that vibrationally AADA is cooled less efficiently.

As would be expected, the excitation spectra of ABCO and AADA qualitatively have the same appearance: the "cage squashing" mode ν_{14}, whose frequency is slightly reduced in comparison with that of the analogous mode ν_{12} in ABCO (618.8 *vs* 626.1 cm^{-1}), is the dominant vibration in the spectrum. Apparently, excitation of a lone-pair electron in AADA is accompanied by the same kind of geometry changes as observed

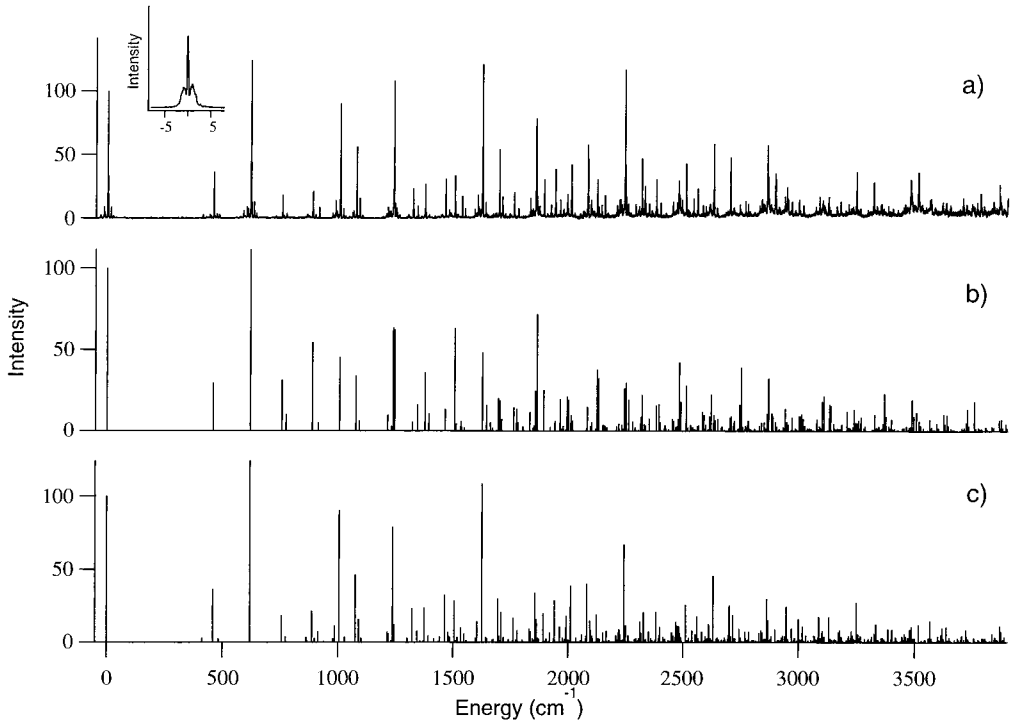

Figure 4. Excitation spectrum of the $S_1 \leftarrow S_0$ transition of 1-azaadamantane. The excitation energy is given with respect to the energy of the 0−0 transition located at 37 725 cm^{-1}. (a) Experimentally observed fluorescence excitation spectrum. (b) Spectrum predicted by employing Franck−Condon factors for transitions from the zero-point level in S_0 to a_1 levels in S_1, and which have been calculated from the B3LYP/6-311G* equilibrium geometries and force fields of S_0 and D_0. (c) Spectrum predicted by employing the equilibrium geometry of S_1 as it was reconstructed from the experimentally observed intensities of the $\nu_i(a_1)^1_0$ transitions. This spectrum also contains, apart from transitions to a_1 levels, transitions to e levels (see text).

for ABCO. The observation that the 0−0 transition is not the strongest band in the excitation spectrum suggests, however, that these geometry changes are somewhat larger in AADA than in ABCO. We notice moreover that for ABCO several other modes, such as ν_{11} (bending of $C_1NC_{1'}$ and $C_1C_2C_3$), ν_9 (C_1C_2 stretch), ν_8 (cage deformation), and ν_7 (CH_2 wagging), were found to be important. For AADA the only other dominant activity is found in the mode at 1005.9 cm^{-1} and to a lesser extent in the mode at 457.3 cm^{-1}, which will be identified (*vide infra*) as the ν_{10} (cage deformation) and ν_{15} (torsion cyclohexyl moiety) modes.

The lowest excited singlet state of AADA arises from excitation to a 3s Rydberg orbital. Considering that the excitation spectrum of the $S_1 \leftarrow S_0$ transition in ABCO could be successfully modeled by employing for S_1 the equilibrium geometry and force field of the ground state of the radical cation, a similar approach is expected to be appropriate for the $S_1 \leftarrow S_0$ excitation spectrum of AADA. To this purpose equilibrium geometries and force fields of the $S_0(1\ ^1A_1)$ ground state of the neutral molecule and the $D_0(1\ ^2A_1)$ ground state of the radical cation of AADA have been calculated at the (U)B3LYP/6-311G* level. The geometrical parameters calculated for these two states are given in Table 4, while vibrational frequencies are listed and compared with experimental frequencies in Table 5. Similar to ABCO, the most important differences between the two geometries can be explained by the change in hybridization of the nitrogen atom upon removal of a lone pair electron. As a result, the apex angle $C_1NC_{1'}$ increases from 109.6° in the neutral to 115.1° in the radical cation, while the angle NC_1C_2 decreases by 7.1°. These changes are slightly greater than in ABCO: although the rigid cage does not permit the amino group to become planar, AADA appears a little easier to flatten than ABCO. It is perhaps interesting to compare the structure of the radical cation of AADA with that of the carbocation analogue 3,5,7-trimethyl-1-adamantyl cation.[46,47] In the latter the angles around the electron-deficient center increase to 117.8°, and the C^+CC angles decrease to 100°: the carbocation center (with a completely vacant p-orbital) has a much greater tendency to flatten than an amine radical cation.

Table 4. Selected Geometrical Parameters (Å and deg) of the Equilibrium Geometries Calculated at the B3LYP/6-311G* Level for the $S_0(1\ ^1A_1)$ Ground State of Neutral AADA and the $D_0(1\ ^2A_1)$ Ground State of the Radical Cation[a]

	$S_0(1\ ^1A_1)$	$D_0(1\ ^2A_1)$	$S_1(2\ ^1A_1)$
$N-C_1$	1.473	−0.024	−0.012
C_1-C_2	1.544	0.037	0.010
C_2-C_3	1.543	−0.005	−0.002
C_1-H_1	1.096	−0.006	0.002
C_2-H_2	1.097	−0.004	−0.001
C_3-H_3	1.097	−0.003	0.000
$C_1NC_{1'}$	109.6	5.5	6.0
NC_1H_1	108.3	1.6	0.4
NC_1C_2	111.7	−7.1	−7.0
$C_1C_2H_2$	109.8	−2.8	−2.3
$C_1C_2C_3$	108.6	−0.7	0.0
$C_2C_3H_3$	110.4	−0.9	−1.0
$C_2C_3C_{2'}$	109.0	0.7	0.4

[a] The parameters as reported for the geometry of the lowest excited singlet state of the neutral molecule have been obtained by employing the observed intensities of the $\nu_i(a_1)^1_0$ transitions in the $S_1 \leftarrow S_0$ excitation spectrum. Parameters given for D_0 and S_1 are given as changes with respect to the geometry of S_0.

The frequencies calculated for the S_0 state of AADA are in excellent agreement with the data obtained from IR[8] and previously[8] and presently obtained Raman spectra. The same tendency is found as in ABCO: the low frequencies are only slightly overestimated, but the deviations (average 1.6%) increase with frequency up to 4%. The standard linear scaling procedure here gives a root-mean-square error of 9 cm^{-1}, and a largest error of 28 cm^{-1}. Interestingly, the frequencies calculated for the lowest-frequency a_2 torsional modes of ABCO

(46) Laube, T. *Angew. Chem., Int. Ed. Engl.* **1986**, *25*, 349.
(47) Laube, T.; Schaller, E. *Acta Crystallogr. Sect. B* **1995**, *51*, 177.

Table 5. Experimental and Calculated (B3LYP/6-311G*) Fundamental Vibrational Frequencies (cm^{-1}) of a_1 and e Vibrations in the Ground and First Excited States of AADA and Intensities in the $S_1 \leftarrow S_0$ Excitation Spectrum[a]

		vibrational frequencies				intensities	
		S_0(exp)	S_0(calc)	S_1(exp)	D_0(calc)	I(exp)	I(calc)[b]
a_1	ν_{15}	434	440	457.3	460.2	36	30
	ν_{14}	598	604	618.8	632.3	124	113
	ν_{13}	767	766	756.3	759.6	18	32
	ν_{12}	785	794	773.6	791.7	4	10
	ν_{11}	936[c]	941	887.0	891.5	22	55
	ν_{10}	1040[d]	1056	1005.9	1021.1	90	46
	ν_9	1095	1119	1090.3	1096.2	16	6
	ν_8	1307	1332	1244.2	1286.1	12	64
	ν_7	1360	1400	1322.5	1365.8	23	6
	ν_6	1476	1507	1487.4[e]	1516.7	5	1
	ν_5	1495	1531		1549.5		3
e	ν_{46}	327	333		344.3		
	ν_{45}	409	415	410.6	405.3	3	
	ν_{44}	469	471	481.6[g]	476.9	3	
	ν_{43}	666	675		646.7		
	ν_{42}	797	802		774.3		
	ν_{41}		908	863.6	863.6	4	
	ν_{40}	915	921	899.7[g]	905.7	3	
	ν_{39}	991[f]	995	979.0	984.7	3	
	ν_{38}	1040[d]	1058	985.3	992.1	11	
	ν_{37}	1108	1131	1101.1	1117.2	3	
	ν_{36}	1186	1210		1178.4		
	ν_{35}	1275	1306	1219.5	1254.5	6	
	ν_{34}	1318	1344	1301.7[h]	1332.3	3	
	ν_{33}	1332	1358	1301.7[h]	1339.9	3	
	ν_{32}	1345	1385	1375.2[i]	1384.0	15	
	ν_{31}		1404	1375.2[i]	1401.7	15	
	ν_{30}	1437	1495	1478.8[g]	1494.4	7	
	ν_{29}		1509	1485.3[g]	1510.7	4	

[a] Intensities are given relative to the intensity of the 0−0 transition, which is taken as 100. [b] Calculated by using the equilibrium geometry and force field of the ground state radical cation. [c] Reference 8 identifies a band observed at 981 cm^{-1} with ν_{11}. This would in the present study imply a scaling factor of 1.043, which is completely outside the range of scaling factors observed for other vibrations. [d] Reference 8 identifies a band observed at 991 cm^{-1} with ν_{10}. This would in the present study imply a scaling factor of 0.938, which deviates significantly from the scaling factors observed for the other vibrations. Considering that the calculations predict similar frequencies for $\nu_{10}(a_1)$ and ν_{38}(e), the band observed at 1042 cm^{-1} cannot be assigned unambiguously to either one of them. [e] The 6^1_0 transition cannot be identified unambiguously. Its intensity has consequently not been employed in the reconstruction of the equilibrium geometry of the excited state from observed intensities of $\nu_i(a_1)^1_0$ transitions. [f] Raman spectra actually show two bands at 981 and 991 cm^{-1}. Although ν_{39} is here rather arbitrarily assigned to the 991-cm^{-1} band, it is not clear how the other band should be assigned. [g] Although hot bands cannot completely explain the presence of every one of the various close-lying peaks in these regions, the proposed assignment and certainly reported intensity remain tentative on account of the presence of these hot bands. [h] The band at 1301.7 cm^{-1} can be attributed to either the 34^1_0 or the 33^1_0 transition. [i] The band at 1375.2 cm^{-1} can be attributed to either the 32^1_0 or the 31^1_0 transition.

(73 cm^{-1}) and AADA (318 cm^{-1}) are significantly different, showing that AADA is more rigid in this respect.

The $S_1 \leftarrow S_0$ excitation spectrum predicted on the basis of these equilibrium geometries and force fields is depicted in Figure 4b. In general, good agreement is observed with the experimental spectrum of Figure 4a, allowing us to come to a conclusive assignment of the transitions involving a_1 vibrations. The only a_1 vibrations that cannot be identified unambiguously are ν_6 and ν_5: the 6^1_0 and 5^1_0 transitions are predicted to have a low intensity, and to be located in regions where several combination bands and hot bands are expected. The minor differences encountered between observed and calculated frequencies of overtones and combination bands once again indicate that the potential energy surface of the first excited singlet state is quite harmonic.

In the analysis of the $S_1 \leftarrow S_0$ excitation spectrum of ABCO it was concluded that several e vibrations are active. A similar situation might in principle occur for AADA. Indeed, several distinct bands are present in the spectrum that cannot be attributed to transitions to a_1 levels, but must derive from transitions to e levels. Some of the $\nu_i(e)^1_0$ transitions are easily identified, but as the less efficient vibrational cooling encountered in our experiments on AADA results in a larger number of hot bands than in ABCO, assignments such as the 44^1_0, 40^1_0, 30^1_0, and 29^1_0 transitions should be considered as tentative. The ν_{34} and ν_{33} modes are calculated to be so close in frequency (1332 and 1340 cm^{-1}) that a specific assignment of the 1301.7-cm^{-1} band to one of them is unwarranted. A similar uncertainty occurs in the assignment of the 1375.2-cm^{-1} band to the 32^1_0 or 31^1_0 transition, modes for which frequencies of 1384 and 1402 cm^{-1} have been calculated.

The frequencies of a_1 and e vibrations in the lowest excited singlet state are given in Table 5. This table also contains the observed intensities of the $\nu_i{}^1_0$ transitions and for the a_1 vibrations the intensity predicted on the basis of the equilibrium geometries and force fields of S_0 and D_0. The correspondence between computed (scaled) frequencies for the radical cation and the fundamental transition energies in the excitation spectrum is quite good, with a root-mean-square error of 11 cm^{-1} and largest error of 21 cm^{-1}.

As for ABCO, we thus come to the conclusion that one of the prominent features of the $S_1 \leftarrow S_0$ excitation spectrum of AADA is the activity of e vibrations as the result of vibronic coupling with states of E symmetry. In AADA the $3p_{x,y}(1\ ^1E)$ state is located at 42 280 cm^{-1} [45] (42 247 cm^{-1} was reported previously).[27] Comparison of the energy difference with the lowest excited singlet state (4555 cm^{-1}) with that in ABCO (4658 cm^{-1}) and the observation that, similar to ABCO, the oscillator strength of the $S_2 \leftarrow S_0$ transition of AADA is an order of magnitude larger than that of the $S_1 \leftarrow S_0$ transition[45] indeed corroborate a similar role of vibronic coupling in both compounds. The role of vibronic coupling in AADA with the $3p_z(3\ ^1A_1)$ Rydberg state *via* a_1 vibrations might, on the other hand, be different. Although the energy gap between the S_1 and S_3 states is about the same for ABCO and AADA (5298 and 5073 cm^{-1},[33,45] respectively), fluorescence excitation spectroscopy on the S_2 and S_3 states in AADA[45] shows that the oscillator strengths of the transitions to these two states are in the ratio of about 14:1, which is significantly different from the ratio found for ABCO (3:1). If vibronic coupling between S_1 and S_3 plays a role at all, these observations would indicate that the intensities of transitions to a_1 levels would be less influenced in the $S_1 \leftarrow S_0$ excitation spectrum of AADA than in that of ABCO.

Under the assumption that the force field of S_1 is the same as the force field of D_0, our calculations have shown that considerable normal mode rotation occurs upon excitation of ABCO. The Duschinsky matrix calculated for the a_1 vibrations of AADA and given in Table 6 shows that mode mixing is also present here, but to a lesser extent. The only two modes, which become heavily scrambled upon excitation, are ν_6 and ν_5.

It can be concluded from Table 5 that the Franck−Condon calculations predict the intensity distribution among the various a_1 modes reasonably well for AADA. Nevertheless, the differences with the experimentally determined intensities are observed to be larger than in ABCO, where in effect only the prediction for mode ν_{11} showed some deviation. Use of the experimentally determined intensities of the $\nu_i(a_1)^1_0$ transitions with the exception of 6^1_0 and 5^1_0, which could not be assigned unambiguously, allows us to determine what differences between the geometry of S_1 and D_0 would be implied if these intensity

Table 6. Duschinsky Matrix for the a_1 Vibrations in AADA Calculated from the Force Fields of the Ground State of the Neutral Molecule and the Radical Cation[a]

	D_0										
S_0	ν_{15}	ν_{14}	ν_{13}	ν_{12}	ν_{11}	ν_{10}	ν_9	ν_8	ν_7	ν_6	ν_5
ν_{15}	**0.997**	0.061	−0.032	−0.014	0.003	−0.003	0.007	0.006	0.005	0.002	−0.001
ν_{14}	−0.064	**0.990**	−0.050	−0.063	0.070	−0.054	0.027	0.029	0.007	0.005	0.018
ν_{13}	0.030	0.064	**0.918**	**0.370**	0.117	0.026	0.013	0.024	−0.014	0.007	−0.004
ν_{12}	−0.001	0.055	**−0.360**	**0.917**	−0.122	0.099	−0.030	0.001	−0.007	−0.005	0.015
ν_{11}	−0.002	−0.061	−0.143	0.060	**0.970**	0.127	−0.084	−0.077	0.032	0.005	0.004
ν_{10}	−0.003	0.040	0.015	−0.099	−0.081	**0.941**	**0.289**	0.102	0.037	0.005	0.033
ν_9	−0.004	−0.039	−0.034	0.060	0.090	**−0.254**	**0.944**	−0.172	0.003	−0.004	−0.024
ν_8	−0.004	−0.045	−0.041	0.013	−0.100	−0.119	0.127	**0.939**	**−0.269**	−0.003	0.037
ν_7	−0.005	−0.020	0.004	0.017	−0.001	−0.073	0.024	**0.259**	**0.959**	−0.009	0.083
ν_6	0.001	−0.017	0.002	−0.004	−0.005	−0.025	0.007	−0.044	−0.048	**0.674**	**0.735**
ν_5	−0.004	0.007	−0.012	0.008	−0.003	0.014	−0.003	0.046	0.053	**0.739**	**−0.670**

[a] Dominant contributions are given in bold.

differences derive exclusively from this geometry factor. In an analogous way as has been done for ABCO (*vide supra*), geometrical parameters have been derived for S_1, which are given in Table 4. As might be expected, the corrections, which need to be applied to account for the observed intensity distribution of the $\nu_i(a_1)^1_0$ transitions, are somewhat larger than those calculated for ABCO. The $S_1 \leftarrow S_0$ excitation spectrum predicted on the basis of the calculated equilibrium geometry for the lowest excited singlet state is depicted in Figure 4c. Employing the same approach as for the construction of Figure 2c, this spectrum also contains the transitions to levels of e symmetry. Comparison with the experimental spectrum (Figure 4a) shows that the calculations now predict the intensities of the dominant overtones and combination bands significantly better than in the first model (Figure 4b).

We recall that in principle the differences between the original model calculation and the experimental spectrum might also (in part) be explained by vibronic coupling *via* a_1 vibrations, and the fact that the force fields of S_1 and D_0 need not necessarily be the same. For ABCO the predicted $\nu_i(a_1)^1_0$ intensities deviated only slightly from the observed intensities. In the extreme case that this would be completely attributed to vibronic coupling, the argument that vibronic coupling *via* a_1 vibrations is expected to be of more influence for ABCO than for AADA (*vide supra*) suggests that vibronic coupling cannot be the principal reason for the observed differences for AADA. The same conclusion can be drawn with respect to a possible difference between the force fields of S_1 and D_0, which would imply that the employed Duschinsky matrix differs from the real S_0-S_1 Duschinsky matrix. Model calculations, in which we have tried to account for the observed intensity pattern by adjusting the Duschinsky matrix, lead to the inevitable conclusion that in that case unrealistically large normal mode rotations would be required. These considerations consequently indicate that in AADA the primary cause for the deviations between experimental and theoretical intensities should be looked for in the differences between the equilibrium geometries of S_1 and D_0, and that these differences are larger than those in ABCO.

One of our incentives to study the ground state of the radical cation of AADA *via* spectroscopic studies of the first excited singlet state was that this molecule forms the donor part of a number of important intramolecular electron-donor−acceptor molecules. An important parameter in the theory of electron transfer is the multidimensional set of Franck−Condon factors, which enters into the transition rate expressions based upon Fermi's Golden Rule.[1] From a conceptual point of view, the data available from the present study for the donor part are consequently "complete" since exactly these Franck−Condon factors have been determined here. Historically, however, the relevant Franck−Condon factors are commonly expressed in terms of (mode-resolved) reorganization energies accompanying the changes in geometry upon excitation to the charge-transfer state,[1] although such a transformation in general involves a number of (simplifying) assumptions. The mode-specific reorganization energies and the total reorganization energy obtained from the present studies are given in Table 7. Calculation of the total reorganization energy accompanying ionization of AADA by taking the difference between the computed vertical and relaxed ionization energies leads to a value of 3268 cm^{-1}. The favorable agreement with the same quantity derived from the dimensionless displacement parameters allows the conclusion that the a_1 normal coordinates of AADA in S_0 and D_0 do not exhibit large deviations from harmonicity. The same conclusion was reached in the analysis of overtones and combination bands in the $S_1 \leftarrow S_0$ excitation spectrum.

Table 7. Mode-Specific Reorganization Energies λ_i (cm^{-1}) Calculated for AADA[a]

mode	$\lambda_i(S_0)$[b]	$\lambda_i(D_0)$[c]	λ_i[d]
ν_{15} (434)	172	151	106 (460)
ν_{14} (598)	671	738	293 (563)
ν_{13} (767)	26	229	41 (758)
ν_{12} (785)	212	72	163 (794)
ν_{11} (936)	518	459	262 (931)
ν_{10} (1040)	531	445	505 (1032)
ν_9 (1095)	0	66	–
ν_8 (1307)	834	762	270 (1239)
ν_7 (1360)	14	65	149 (1296)
ν_6 (1476)	76	7	–
ν_5 (1495)	14	30	–
$\sum\lambda_i$	**3068**	**3024**	**1789**

[a] The first column gives the number of the a_1 mode and, in parentheses, its frequency (cm^{-1}) in S_0 as determined experimentally (see Table 5). The last column contains tentative assignments of reorganization energies as determined for normal modes of **1** (Figure 1)[7] to modes of isolated AADA. The dashed entries in this column indicate that the reorganization energy of that particular mode has not been reported. [b] Employing normal coordinates and experimental vibrational frequencies of S_0. [c] Employing normal coordinates of D_0 and experimental vibrational frequencies of S_1. [d] Determined from resonance Raman spectroscopy on **1**.[7] The number in parentheses refers to the reported experimental frequency (cm^{-1}) of the normal mode in **1** corresponding to that of AADA (column 1).

In Table 7 an attempt is made to correlate the mode-specific reorganization energies determined here for isolated AADA with those determined from resonance Raman spectroscopy for normal modes of the electron-donor−acceptor compound **1**.[7] It is clear that such a comparison should be considered with the necessary caution. First of all, the normal modes of the AADA unit incorporated into the electron-donor−acceptor system will be influenced by the presence of the acceptor part. Secondly, the mode-specific reorganization energies determined in ref 7 have been obtained under the assumption that the normal modes and their frequencies do not change upon excitation to the

charge-transfer state, *i.e.*, no Duschinsky mixing occurs. Tables 5 and 6 demonstrate that for isolated AADA these assumptions, in particular the absence of Duschinsky mixing, might be questioned. Indeed, it is seen from Table 7 that the use of S_0 normal coordinates leads to reorganization energies which are significantly different from those determined by employing D_0 normal coordinates. This may not be physically very significant, because the Franck−Condon weighted density of states, which enters into the theoretical expressions for electron transfer, is mostly sensitive to the *total* internal reorganization energy, not so much to the partitioning over the different vibrational modes. Although the data given in Table 7 indicate that for the donor part the *mode-specific* reorganization energies accompanying the charge transfer transition from the ground state are different from those of the charge recombination to the ground state, the total reorganization energy is virtually the same for both transitions. In this respect, the rigid cage amine AADA differs from more flexible molecules such as *N*,*N*,*N*′,*N*′-tetramethyl-*p*-phenylenediamine, in which the reorganization energy accompanying charge recombination is considerably smaller than that of charge separation.[15,48]

A more serious discrepancy between our results on AADA and those of the Raman study on **1** is that the total reorganization energy in the latter is much smaller. The comparison presented in Table 7 implicitly assumes that the resonant state in the Raman experiments on the electron-donor−acceptor compound **1** is characterized by a complete separation of charge. It is well-known[49,50] that the CT transitions in compounds such as **1** derive much of their intensity from mixing with locally excited states. However, considering the results for closely related systems,[49,50] it does not seem very likely that this mixing reduces the CT character enough to explain the ca. 40% smaller reorganization energy. We note that Phillips et al.[7] had to assume fairly large solvent contributions to the total reorganization energy to account for the absorption and fluorescence spectra of **1**, which may be an indication that their experimental approach leads to an underestimation of λ_i.

Despite the limitations mentioned, it is gratifying to see that the mode-specific reorganization energies determined in the present study agree qualitatively well with those determined from the resonance Raman study on the electron-donor−acceptor compound **1**. The donor modes that are most active in the CT transition in **1** also have large displacements in the $D_0 \leftarrow S_0$ transition in AADA.

IV. Conclusions

We have shown that the $S_1 \leftarrow S_0$ fluorescence excitation spectra of ABCO and AADA measured in the present study can be well modeled on the basis of DFT calculations on the ground states of the neutral molecule and its radical cation. Calculations on the latter state have been used to model geometric and vibrational properties of the Rydberg excited state. This approximation turns out to work impressively well, not only with respect to the frequencies of the vibrations, but also with respect to the intensities of the various vibronic transitions to vibrational levels of a_1 symmetry in the excited state. Apart from an unambiguous analysis of transitions to totally symmetric vibrational levels in the excited state, the combination of the experimental excitation spectra and the results of the DFT calculations have enabled us as well to show that the first excited singlet state of both molecules is subject to vibronic coupling with higher-lying Rydberg states.

When the intensities of fundamental $\nu_i(a_1)^1_0$ transitions are used to predict the geometry change upon excitation, still using the radical cation force field, a semiempirical estimate of the S_1 geometry can be made. This turns out to differ only slightly from the computed D_0 structure. On the basis of this calculated S_1 geometry, a more accurate prediction is possible of the intensities in the whole spectrum, *i.e.*, including combination bands. It should be kept in mind that the theory employed to calculate intensities has its limitations. In view of this, the difference between the radical cation structure of ABCO and the semiempirically determined S_1 structure is hardly significant. For AADA, the radical cation model seems to be somewhat less adequate.

The results obtained for AADA have been employed to determine the mode-specific reorganization energies associated with the $D_0 \leftarrow S_0$ transition. These energies have been shown to compare qualitatively well with those determined by resonance Raman spectroscopy for the charge-transfer transition of an electron-donor−acceptor molecule, in which AADA serves as the donor part. At the same time, however, this analysis has revealed the pitfalls one should be aware of in the analysis of reorganization energy, *e.g.*, Duschinsky rotation of normal coordinates upon excitation, which is generally neglected, has been found in the present case to have a significant influence. The total reorganization energy derived from the Raman experiments on **1** is considerably smaller than that found in the present work for ionization of AADA.

From our studies it can be concluded that the equilibrium geometries and force fields of the first excited singlet states are essentially the same as those of the ground state of the radical cation. This implies that the excitation spectra of higher excited singlet states, which, like S_1, are Rydberg states converging upon the electronic ground state of the radical cation, should be very similar to the excitation spectrum of S_1. The extent to which the equilibrium geometries and force fields of S_1 and D_0 are similar might in principle be investigated in even more detail by high-resolution studies of the $D_0 \leftarrow S_1$ transition by using techniques such as ZEKE-PFI spectroscopy. For ABCO and AADA, studies along both approaches are presently being performed.

Acknowledgment. The authors wish to thank Prof. J. W. Verhoeven for valuable suggestions and discussions, for providing a preprint of ref 8, and for critical reading of the manuscript. We thank Prof. C. A. de Lange for use of equipment and Dr. J. W. Hofstraat and Dr. B. Rossenaar (AKZO Nobel, Arnhem) for measuring the FT-Raman spectra of ABCO and AADA. This research was sponsored by the "Stichting Nationale Computer Faciliteiten" (National Computing Facilities Foundation, NCF) for the use of supercomputer facilities and supported (in part) by the Netherlands Foundation for Chemical Research (SON), with financial support from the Nederlandse Organisatie voor Wetenschappelijk Onderzoek (Netherlands Organization for Scientific Research, NWO).

JA972411U

(48) Nelsen, S. F.; Yunta, M. J. R. *J. Phys. Org. Chem.* **1994**, *7*, 55.
(49) Bixon, M.; Jortner, J.; Verhoeven, J. W. *J. Am. Chem. Soc.* **1994**, *16*, 7349.
(50) Verhoeven, J. W.; Scherer, T.; Wegewijs, B.; Hermant, R. M.; Jortner, J.; Bixon, M.; De Paemelaere, S.; De Schryver, F. C. *Recl. Trav. Chim. Pays-Bas* **1995**, *114*, 443.